CT texture analysis in colorectal liver metastases and the surrounding liver parenchyma and its potential as an imaging biomarker of disease aggressiveness, response and survival

European Journal of Radiology 102 (2018) 15–21

Contents lists available at ScienceDirect

European Journal of Radiology

journal homepage: www.elsevier.com/locate/ejrad

Research Article

CT texture analysis in colorectal liver metastases and the surrounding liver parenchyma and its potential as an imaging biomarker of disease aggressiveness, response and survival

R.C.J. Beckers[a,b,c,d], S. Trebeschi[a,b], M. Maas[b], R.S. Schnerr[c], J.M.L. Sijmons[e], G.L. Beets[a,f], J.B. Houwers[c], R.G.H. Beets-Tan[a,b], D.M.J. Lambregts[b,*]

[a] GROW School for Oncology and Developmental Biology, Maastricht University Medical Centre, P.O. Box 616, 6200 MD, Maastricht, The Netherlands
[b] Department of Radiology, The Netherlands Cancer Institute, P.O. Box 90203, 1006 BE, Amsterdam, The Netherlands
[c] Department of Radiology, Maastricht University Medical Center, P.O. Box 6200, 6202 AZ, Maastricht, The Netherlands
[d] Department of Surgery, Maastricht University Medical Center, P.O. Box 6200, 6202 AZ, Maastricht, The Netherlands
[e] Faculty of Health, Medicine and Life Sciences, Maastricht University, P.O. Box 6200, 6202 AZ, Maastricht, The Netherlands
[f] Department of Surgery, The Netherlands Cancer Institute, PO Box 90203, 1066 CX, Amsterdam, The Netherlands

ARTICLE INFO

Keywords:
Tomography
Spiral computed
Colorectal neoplasms
Liver
Neoplasm metastasis
Radiographic image enhancement
Texture analysis

ABSTRACT

Objectives: To study the ratio between the CT texture of colorectal liver metastases (CRLM) and the surrounding liver parenchyma and assess the potential of various texture measures and ratios as predictive/prognostic imaging markers.

Materials: Seventy patients with colorectal cancer and synchronous CRLM were included. All visible metastases, as well as the whole-volume of the surrounding liver, were separately delineated on the portal venous phase primary staging CT. Texture features entropy (E) and uniformity (U) were extracted and ratios between the texture features (T) of the metastases and background liver ($T_{metastases}/T_{liver}$) calculated. Texture features were compared with clinical outcome parameters: [1] extent of disease (i.e. number of metastases), [2] response to chemotherapy (in 56/70 patients who underwent chemotherapy and CT for response evaluation), and [3] overall survival.

Results: The $E_{metastases}/E_{liver}$ ratio was lower in patients with limited disease ($P = 0.02$) and associated with overall survival, albeit not statistically significant when tested in multivariable analyses (HR 1.90; $P = 0.07$); $U_{metastases}/U_{liver}$ was higher in patients with limited disease ($P = 0.02$). $E_{metastases}$ showed a trend towards a higher value in patients that responded well to chemotherapy ($P = 0.08$).

Conclusion: The ratio between the texture of liver metastases and the surrounding liver appears to reflect relevant changes in tissue microarchitecture and may be of value to assess the extent of disease and help predict overall survival.

1. Introduction

Colorectal cancer is one of the most common cancers worldwide [1]. Approximately 15–25% of all patients have colorectal liver metastases (CRLM) at the time of diagnosis [2–4]. These synchronous CRLM patients tend to have a poor prognosis with a reported 1-year survival of less than 30% and a 5-year survival of less than 5% when untreated, with 5-year survival rates of up to 60% in selected groups that can undergo curative surgical resection [3].

Imaging plays a crucial role in the diagnosis and follow-up of CRLM. In many institutions, contrast-enhanced CT remains the primary modality for the staging of patients with colorectal cancer [5], although MRI is increasingly applied because of its superiority in detecting small liver metastases [6]. To date, the mainstay of imaging assessment consists of a visual assessment of lesions and changes in size and morphology as a result of the response to therapy. The most widely adopted method to evaluate treatment response is Response Evaluation Criteria in Solid Tumours (RECIST), which provides standardised measures of response in terms of lesion size [7]. Although commonly used in clinical trials and daily practice, RECIST is known to have significant limitations as

Abbreviations: CAPOX, capecitabine + oxaliplatin; CRLM, colorectal liver metastases; CT, computed tomography; E, entropy; HR, hazard ratio; LoG, Laplacian of Gaussian; MRI, magnetic resonance imaging; PVP, portal venous phase; RECIST, Response Evaluation Criteria in Solid Tumours; U, uniformity; VOI, volume of interest

* Corresponding author at: Dept. of Radiology, The Netherlands Cancer Institute P.O Box 90203, 1066 CX, Amsterdam, The Netherlands.
E-mail address: d.lambregts@nki.nl (D.M.J. Lambregts).

https://doi.org/10.1016/j.ejrad.2018.02.031
Received 2 November 2017; Received in revised form 10 January 2018; Accepted 26 February 2018

size measurements fail to capture (micro-)structural changes related to for example intralesional perfusional or necrotic changes, which are known to be significant factors associated with therapeutic response [7–9].

Therefore, there is nowadays a growing interest in the use of quantitative imaging and image postprocessing techniques to gain a more profound insight into the tumour biology. One of such techniques is texture analysis, which is a mathematical approach that uses an algorithm to quantify tissue heterogeneity by assessing the distribution of coarseness and irregularity of pixel intensities within a volume of interest (VOI) derived from a lesion or organ on an image [10]. In patients with CRLM, texture analysis has been studied using both CT and MRI data, although most evidence so far exists for CT. So far, two main settings have been explored: one group of studies focused on the intralesional texture of the liver metastases itself, which was found to significantly correlate with the response to chemotherapy, as well as with survival [11–14]. Other studies focused not on the texture of the metastases, but on that of the surrounding apparently disease free liver parenchyma and showed that diffuse parenchymal textural changes may hold promise as a prognostic marker to assess and even predict the occurrence of metastatic disease in the liver [15,16]. Although the texture of both liver metastases and surrounding liver have been studied, to our knowledge there have been no reports so far studying the relation between the two. This would be worthwhile to study as it may potentially provide valuable insights into the relation between texture findings and underlying tumour behaviour.

The aim of our study is twofold: first, we aim to explore the relation between the CT texture of CRLM and the surrounding liver parenchyma and assess if the ratio between the two may be of added value as a predictive or prognostic imaging marker. Second, we want to investigate whether we can confirm results of previous studies that CT texture analysis has a potential value as a biomarker of disease aggressiveness, response and survival in patients with CRLM.

2. Materials and methods

2.1. Patients

Eighty-three consecutive patients with CRLM treated at [Maastricht University Medical Center] between April 2008 and December 2013 were considered for inclusion in this retrospective study. The study was approved by the institutional ethical review board; due to the retrospective nature, informed consent was not required. Inclusion criteria were as follows: *(a)* histopathologically confirmed primary (non-recurrent) colorectal adenocarcinoma; *(b)* availability of a primary staging CT including (at least) a portal venous phase (PVP); *(c)* presence of at least one synchronous CRLM at the time of diagnosis and staging; *(d)* no previous liver surgery; *(e)* no previous chemotherapy and *(f)* no clinical or imaging evidence of diffuse liver diseases such as steatosis or cirrhosis. Thirteen patients were excluded because of the presence of concomitant second malignancies at the time of diagnosis (n = 3), inadequate CT contrast timing (n = 3), and the presence of diffuse hepatic metastases, leaving too little 'normal' liver parenchyma to delineate (n = 7). This left a total study population of 70 patients (50 male/20 female, median age 69, range 39–85) for inclusion; see consort diagram in Fig. 1. Part of the study patients (29/70) were included in a previously published multicentre study cohort, which focussed on whole liver texture analysis to predict metachronous CRLM and therefore does not overlap with the aims of the current study [15].

2.2. CT acquisition

All CT scans were acquired using multi-slice CT equipment (Philips Brilliance 64, Philips Medical Systems, Best, The Netherlands; Siemens Somatom Sensation 16 or Somatom Definition Flash, Siemens Healthcare, Erlangen, Germany). PVP images of the liver/abdomen were obtained with a tube voltage of 100–120 kVp. The contrast medium (Ultravist 300 mgI/ml; Iopromide, Bayer Healthcare, Berlin, Germany) was prewarmed to 37 °C (99°F) and administered intravenously as a bolus injection of 110 ml at a rate of 3.5 ml/s, followed by a saline flush of 40 ml. The scan delay for the PVP was set at 70 s. Images were reconstructed in transverse plane using iterative reconstruction (Siemens Somatom Definition Flash) or filtered back-projection (Philips Brilliance 64/Siemens Somatom Sensation 16) with a soft tissue filter. Slice thickness was 3 or 5 mm.

2.3. Image delineation

All delineations were performed on the primary staging CT. The PVP images were transferred to an offline workstation for delineation, using an open source software tool (MANGO; Multi-image Analysis GUI, version 2.6, Research Imaging Institute, University of Texas Health Science Center, San Antonio, TX). One reader with experience in liver delineation (R.B.) manually delineated per slice *(a)* all visible liver metastases, and *(b)* the surrounding (apparently disease free) liver parenchyma (Fig. 2). Delineations were performed according to methods previously reported [13,15,16]. For the delineation of the surrounding liver, the border of the liver, any visible focal liver lesions (including both benign lesions as well as any metastases), the inferior vena cava, caudate lobe, large hepatic veins, arteries and biliary ducts were excluded from the VOI.

2.4. Texture analysis

2D Texture analysis was performed with an in-house software written in Python (Python Software Foundation, version 2.7, http://www.python.org) by one of the authors (S.T.; who was blinded to all clinical patient data and outcomes) largely based on the open source Python package pyradiomics [17], according to methods previously reported [13,15,16]. The image analysis technique used for this study comprised two main stages: image filtration followed by the quantification of texture. Prior to feature extraction, CT volumes were resampled to isotropy (1 × 1 × 1 mm) using b-spline basis functions, whereas nearest neighbour was used for the delineations. In addition to the original image, the Laplacian of Gaussian (LoG) filter was applied to enhance edges and irregularities at two different resolutions: fine ($\sigma = 0.5$) and coarse ($\sigma = 2.5$). For quantification of the texture, entropy (E) and uniformity (U) were the main parameters that were extracted, similar to previously reported research on texture analysis in CRLM [18]. The meaning of these two features in relation to tissue microarchitecture is schematically illustrated in Fig. 3. Entropy is a measure that gives an indication of the irregularity of the grey-level distribution, while conversely, the uniformity is indicative of its homogeneity. A higher entropy (and low uniformity) typically reflects a more "heterogeneous" distribution of pixels (and thus a more heterogeneous underlying tissue structure) while on the other hand a high uniformity is associated with a more "homogeneous" distribution of pixels (and therefore a more homogeneous tissue structure) [19–21]. Both features were calculated from a histogram, based on the points within the region of interest with a bin size of one Hounsfield unit. For each texture feature the ratio between the metastases and surrounding liver was calculated according to the following formula:

$$\frac{T_{metastases}}{T_{liver}} = T_{ratio}$$

T represents the respective texture features, $T_{metastases}$ represents the VOIs of all visible liver metastases combined for each patient, and T_{liver} represents the VOI of the whole volume of the surrounding liver (excluding the metastases). Total time required to delineate and analyse one patient case was approximately 15 min.

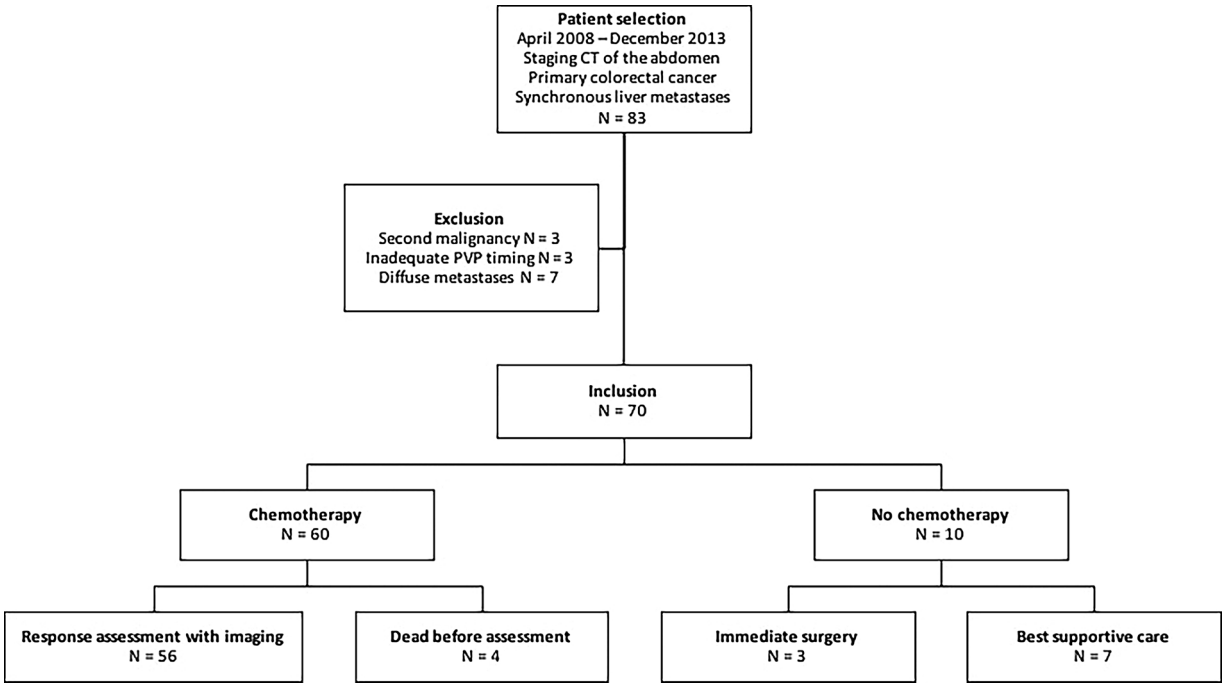

Fig. 1. Flow-chart of the selection, inclusion and treatment of the studied patients.

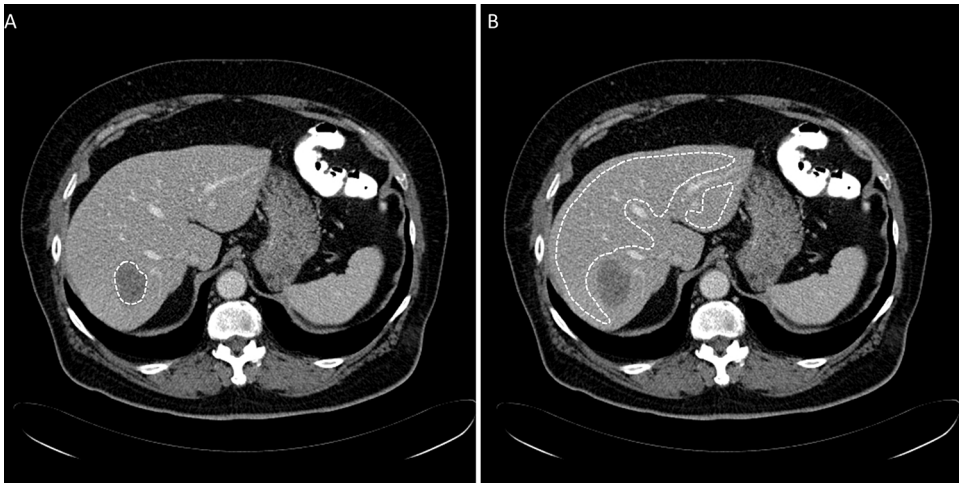

Fig. 2. Delineation of metastatic liver lesions and background liver parenchyma.
Representative example of the initial staging portal venous phase CT image of a patient with a solitary CRLM. The dotted lines represent the delineations used to derive the texture features. (A) shows the delineation of the metastasis, while (B) shows the delineation of the background liver. The border of the liver, any visible lesions, the inferior vena cava and large portal and hepatic veins were excluded. The ratio of the texture features (T) between the metastases and background liver were calculated as $T_{metastases}/T_{liver}$.

2.5. Clinical outcome measures/standard of reference

Texture features were compared with three clinical outcome parameters: (1) extent of disease, (2) response to chemotherapy, and (3) overall survival (OS). For the extent of disease, patients were categorised based on the number of liver metastases visible at the time of diagnosis: patients with ≥5 liver metastases were classified as the 'extensive disease' group and patients with < 5 liver metastases as the 'limited disease' group (a cut-off based on previous literature) [22]. Since not all patients underwent surgical resection of their liver metastases, response to chemotherapy was assessed on post-chemotherapy imaging and patients were categorised according to RECIST 1.1 [7]. Patients with complete response (CR) or partial response (PR) were classified as the 'responders' group and patients with stable disease (SD) or progressive disease (PD) were classified as the 'nonresponders' group. OS was defined as the absence of death during follow-up. Fifty-eight patients died during follow-up, median FU in these patients was 14.5 months (range 1–71). In the twelve patients that were still alive at the time of writing, median FU was 57.5 months (rang 43–103).

2.6. Statistical analysis

Statistical analyses were performed using the Statistical Package for the Social Sciences (IBM Corp. Released 2015. IBM SPSS Statistics for Windows, Version 23.0. Armonk, NY: IBM Corp.). The Shapiro-Wilk Test was used to test for normality. Independent sample T-tests (or Mann-Whitney *U* test in case of non-normally distributed data) were used to compare mean texture features and ratios between *(a)* patients with limited (< 5 liver metastases) versus extensive (≥5 metastases) disease and *(b)* responders versus nonresponders (according to RECIST 1.1). The Holm-Bonferroni correction method was used to correct for multiple testing [23].

The predictive value of texture parameters for OS was assessed by use of multivariable Cox proportional hazards models. With univariable analyses, the potentially predictive factors were identified, which were then entered in the multivariable Cox proportional hazards model. Hazard ratios (HRs) with 95% confidence intervals (CI) were calculated. *P*-values ≤ 0.05 were considered statistically significant.

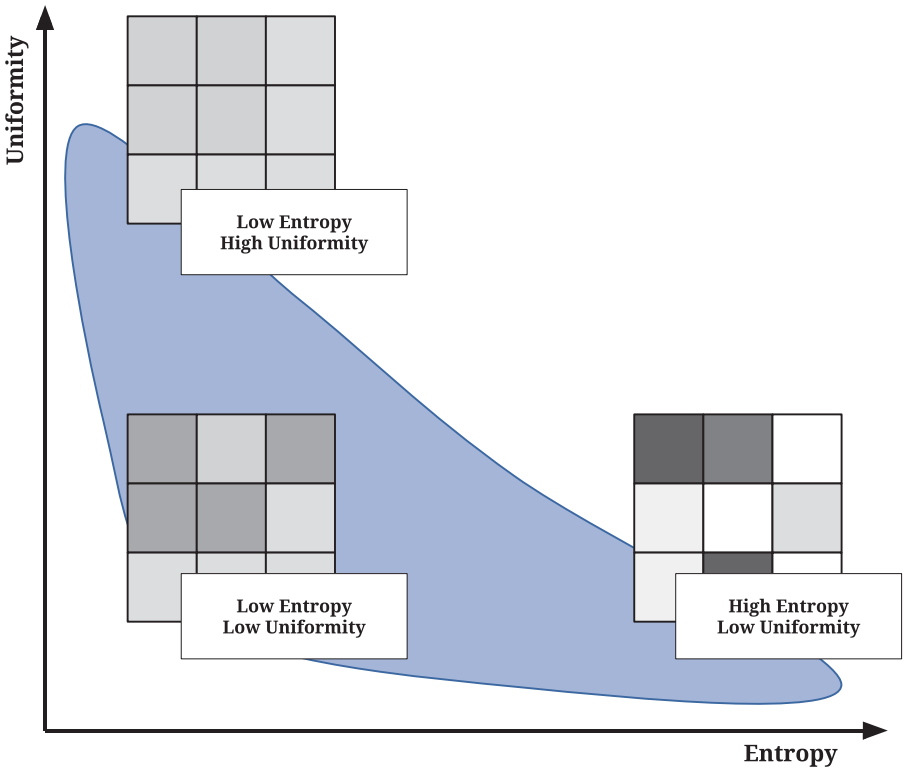

Fig. 3. Relation between entropy and uniformity.
Illustration of the relationship between entropy (E) and uniformity (U) values. Low values of entropy and uniformity are shown in the bottom left with random displacement of few intensity values. As the image becomes more hypo-intense, with only few spots of hyper-intensity, the uniformity increases (upper left) while the entropy remains unaffected. On the other hand, allowing for a range of hyper-intensities which will induce a more irregular, unpredictable pattern (bottom right) the entropy will increase, as the distribution becomes more uncertain.

3. Results

3.1. Patients

Baseline patient characteristics are described in Table 1. The primary tumor site was the rectum in 30 and the colon in 40 patients. The median number of CRLMs per patient was 3 (range 1–20); 42 patients had < 5 metastases (limited disease) and 28 had ≥5 metastases (extensive disease). Three patients underwent immediate surgical resection. Sixty patients underwent neoadjuvant or palliative chemotherapy; the routine neoadjuvant chemotherapeutic regimen (in 80% of patients) consisted of CAPOX with or without the addition of Bevacizumab. In the patients undergoing chemotherapy, response evaluation with imaging (according to RECIST 1.1) was available in 56 patients: 31 were responders (all PR), 25 were nonresponders (17 SD, 8 PD). Median OS was 22,5 months (range 1–102 months).

Table 1
Baseline characteristics.

Patient characteristics	Total N = 70
Age (y)	
Median	69
Range	39–85
Sex	
Male	50 (71.4)
Female	20 (28.6)
Primary tumour site	
Rectum	30 (42.9)
Colon	40 (57.1)
Number of hepatic metastases	
Median	3
Range	1–20
Extrahepatic metastases	
No	36 (51.4)
Yes	34(48.6)
Intra-abdominal only	7 (10)
Extra-abdominal (+/− intra abdominal)	27 (38.6)
Treatment CRLM	
Immediate surgery	3 (4.3)
Chemotherapy & surgery	22 (31.4)
Palliative chemotherapy	38 (54.3)
Best supportive care	7 (10.0)
Chemotherapy regimen	
CAPOX[a] + Bevacizumab	39 (65.0)
CAPOX[a]	9 (15.0)
Capecitabine	7 (11.7)
Other	5 (8.3)

Note: Unless otherwise indicated, data are numbers of patients and data in parentheses are percentages.
[a] CAPOX: capecitabine + oxaliplatin.

3.2. Texture features to assess limited vs. extensive disease

Table 2 compares the texture features and ratios of patients with limited (< 5 lesions) and extensive (≥5 lesions) disease. The ratio for the entropy without filter ($E_{metastases}/E_{liver}$) was significantly lower in patients with limited disease ($P = 0.02$) while correspondingly the ratio for uniformity ($U_{metastases}/U_{liver}$) was significantly higher ($P = 0.02$). The remaining ratios, as well as the separate texture features (E and U) of the metastases and liver itself, did not show statistically significant differences between the two groups ($P = 0.67–1.00$).

3.3. Texture features to assess response vs. nonresponse (RECIST 1.1)

Table 2 compares the texture features and ratios between responders and nonresponders for the 56 patients for whom a RECIST response assessment after neoadjuvant chemotherapy was available. Only the lesion entropy without filter ($E_{metastases}$) showed a trend towards a higher value in responders ($P = 0.08$). None of the other features or ratios resulted in any significant outcomes ($P = 0.48–1.00$).

3.4. Texture features to predict survival

Table 3 shows the results for the univariable analyses. Based on these results, the $E_{metastases}/E_{liver}$ ratio (without filter) was combined with age at diagnosis, chemotherapy (Y/N), number of CRLM, resection

Table 2
Textural features of patients with < 5 or ≥5 lesions and responders and non-responders according to RECIST 1.1.

	< 5 Lesions N = 42	≥5 Lesions N = 28	P^*	Responders N = 31	Nonresponders N = 25	P^*
Without filter						
E_{liver}	6.37 ± 0.24	6.29 ± 0.25	1.00	6.32 ± 0.26	6.34 ± 0.25	1.00
U_{liver}	0.02 ± 0.003	0.02 ± 0.003	1.00	0.02 ± 0.003	0.02 ± 0.002	1.00
$E_{metastases}$	6.57 ± 0.33	6.71 ± 0.24	0.67	6.65 ± 0.26	6.51 ± 0.34	0.08
$U_{metastases}$	0.01 ± 0.003	0.01 ± 0.002	0.94	0.01 ± 0.002	0.01 ± 0.003	1.00
$E_{metastases}/E_{liver}$	1.03 ± 0.05	1.07 ± 0.03	**0.02**	1.05 ± 0.03	1.03 ± 0.06	0.59
$U_{metastases}/U_{liver}$	0.87 ± 0.21	0.74 ± 0.09	**0.02**	0.78 ± 0.11	0.89 ± 0.26	0.48
Fine filter						
E_{liver}	5.15 ± 0.25	5.08 ± 0.25	1.00	5.10 ± 0.27	5.12 ± 0.25	1.00
U_{liver}	0.03 ± 0.006	0.04 ± 0.006	1.00	0.04 ± 0.008	0.04 ± 0.006	1.00
$E_{metastases}$	5.33 ± 0.29	5.27 ± 0.24	1.00	5.31 ± 0.28	5.27 ± 0.25	1.00
$U_{metastases}$	0.03 ± 0.006	0.03 ± 0.005	1.00	0.03 ± 0.006	0.03 ± 0.006	1.00
$E_{metastases}/E_{liver}$	1.04 ± 0.04	1.04 ± 0.02	1.00	1.04 ± 0.03	1.03 ± 0.04	1.00
$U_{metastases}/U_{liver}$	0.87 ± 0.11	0.88 ± 0.06	0.92	0.86 ± 0.08	0.90 ± 0.11	1.00
Coarse filter						
E_{liver}	6.16 ± 0.41	6.11 ± 0.40	1.00	6.19 ± 0.43	6.12 ± 0.41	1.00
U_{liver}	0.03 ± 0.008	0.03 ± 0.009	1.00	0.03 ± 0.008	0.03 ± 0.009	1.00
$E_{metastases}$	5.90 ± 1.20	6.46 ± 0.65	0.94	6.23 ± 0.79	5.82 ± 1.42	1.00
$U_{metastases}$	0.03 ± 0.03	0.02 ± 0.009	1.00	0.02 ± 0.01	0.04 ± 0.04	1.00
$E_{metastases}/E_{liver}$	0.96 ± 0.20	1.06 ± 0.12	0.77	1.01 ± 0.14	0.95 ± 0.23	1.00
$U_{metastases}/U_{liver}$	1.23 ± 1.32	0.72 ± 0.32	1.00	0.90 ± 0.50	1.38 ± 1.63	1.00

Note: Data are the mean ± SD, all measurements were performed on primary staging CT before treatment, significant results are printed in bold.
E: Entropy.
U: Uniformity.
* *P*-values after Holm-Bonferroni correction.

Table 3
Univariable Cox proportional hazards model.

Parameter	HR	95% Confidence Interval	*P*
Without filter			
E_{liver}	0.63	0.23–1.73	0.37
U_{liver}	1.04	0.95–1.15	0.41
$E_{metastases}$	2.59	1.00–6.65	0.05
$U_{metastases}$	0.90	0.80 − 1.00	0.05
$E_{metastases}/E_{liver}$ §	2.51	1.44–4.36	**0.001**
$U_{metastases}/U_{liver}$	0.41	0.24–0.72	**0.002**
Fine Filter			
E_{liver}	0.81	0.30–2.19	0.67
U_{liver}	1.01	0.97–1.05	0.70
$E_{metastases}$	0.96	0.39–2.39	0.93
$U_{metastases}$	1.00	0.96–1.04	0.92
$E_{metastases}/E_{liver}$	1.23	0.73–2.07	0.43
$U_{metastases}/U_{liver}$	0.83	0.50–1.40	0.49
Coarse filter			
E_{liver}	0.91	0.47–1.75	0.77
U_{liver}	1.00	0.97–1.03	0.93
$E_{metastases}$	1.46	1.13–1.89	**0.004**
$U_{metastases}$	0.98	0.96–1.00	**0.012**
$E_{metastases}/E_{liver}$	1.81	1.06–3.09	**0.030**
$U_{metastases}/U_{liver}$	0.49	0.29–0.84	**0.009**
Clinical parameters			
Age§	1.01	0.98–1.04	0.45
Sex	1.09	0.61–1.93	0.78
Location of primary tumour[a]	0.61	0.32–1.18	0.14
Resection of primary tumour†	0.35	0.20–0.62	**0.000**
Chemotherapy†,§	0.26	0.12–0.57	**0.001**
Number of CRLM§	1.06	1.02–1.10	**0.006**
Resection of CRLM†,§	0.20	0.10–0.41	**0.000**
Extrahepatic disease‡,§	1.378	1.04–1.83	**0.025**

Note: Texture ratios are dichotomized based on the median value, according to methods previously reported [34], uniformity values were multiplied by 1000 in line with previous research [15], significant results are printed in bold.
Variables indicated with § were included in the multivariable model. To avoid overfitting and because of a relation to other variables, the remaining significant variables were not included in the multivariable model (e.g. the vast majority of patients who underwent resection of their liver metastases also underwent resection of their primary tumour).
[a] left sided (transversum, descendens, sigmoid or rectum)/right sided (ascendens or caecum).
† No/Yes.
‡ No/abdominal only/extra-abdominal metastases.

Table 4
Multivariable Cox proportional hazards model with entropy ratio.

Parameter	HR	95% Confidence Interval	*P*
$E_{metastases}/E_{liver}$ (without filter)	1.90	0.95–3.78	0.07
Age	1.02	0.99–1.06	0.16
Number of CRLM	1.00	0.96–1.05	0.90
Chemotherapy			
No	1.00		
Yes	0.42	0.18–0.98	**0.044**
Resection of CRLM			
No	1.00		
Yes	0.26	0.11–0.60	**0.004**
Extrahepatic disease			
No	1.00		
Abdominal only	1.12	0.59–2.11	0.74
Extra-abdominal	2.10	0.70–6.29	0.19

Note: Texture ratios were dichotomized based on the median value, according to methods previously reported [34], significant results are printed in bold.
E: Entropy.

of CRLM (Y/N) and the presence of extrahepatic metastases (none/abdominal only/extra-abdominal metastases) in the multivariable model, the results of which are presented in Table 4.

The $E_{metastases}/E_{liver}$ showed a trend towards significance in the multivariable model with a HR of 1.90 (0.95–3.78; $P = 0.07$). Resection of CRLM was an independent predictor of OS (HR 0.26; CI 0.11–0.60; $P = 0.004$), as was chemotherapy (HR 0.42; CI 0.18–0.98; $P = 0.04$).

4. Discussion

The aim of our study was twofold: to test if we could confirm results of previous literature that CT texture analysis has potential value as a predictive imaging marker in patients with CRLM and to get a better insight into the relationship between the texture of CRLM and the surrounding liver architecture. Our results suggest that analysing the ratios between textural changes of the metastases and the surrounding liver parenchyma ($E_{metastases}/E_{liver}$ and $U_{metastases}/U_{liver}$) may be of added value to assess the burden of disease in the liver. Moreover, the texture ratios showed an association with overall survival, albeit it not

statistically significant in multivariate analyses. Finally, we observed a subtle trend towards higher entropy in liver metastases that show a better response to treatment.

As shown in Fig. 3, a more irregular distribution of 'disease' within a certain VOI will typically lead to a higher entropy (and lower uniformity). One can imagine that in the case of a more aggressive disease profile, the liver lesions become more heterogeneous (higher entropy/lower uniformity) while the surrounding liver remains relatively unaffected. This effect on entropy and uniformity in the liver metastases may be highlighted by comparing it to the surrounding liver (as a normalisation factor), which may explain why mainly the ratios were significantly associated with the burden of disease while there was only a subtle, nonsignificant trend for the entropy and uniformity measures itself. An alternative hypothesis would be that the ratio between the texture of the liver metastases and surrounding liver is in itself a unique feature that captures biological properties of the course of metastatic disease within the liver that cannot be identified by looking at either the architecture of the liver lesions or surrounding liver separately.

A higher entropy ratio was also an independent factor that was associated with impaired OS (with a borderline significant HR of 1.90 in multivariate analyses) and may thus be of value as an added biomarker of survival, alongside more well-known clinical predictors such as chemotherapy and resection. This is in line with the findings of previous studies in other tumour types: Ganeshan et al. reported that, for oesophageal cancer, high entropy with a medium to coarse filter was associated with a shorter OS [24]. Hayano et al. also suggested that high entropy with a medium filter was associated with a shorter OS in non-small cell lung cancer [25]. In contrast, other groups found the opposite and reported higher entropy (with a fine filter) to be associated with a better OS in patients with head and neck cancer, oesophageal cancer, and colorectal cancer [26–28]. These seemingly discrepant findings may in part be related to the fact that different studies used different image filters. The use of edge enhancement filters in texture analysis, such as the LoG filter used in this study, is to improve the ability to assess and quantify tissue heterogeneity. Lower filter values highlight small changes in intensity and structures with fine textures, while higher filter values highlight structures with medium and coarse textures in the filtered image [19]. As such, the use of different filters may considerably affect study results. Moreover, these previous studies report on a heterogeneous group of tumour types with various different treatment regimens and inherently different tumour prognostic profiles.

When looking at the texture of the metastatic lesions itself, only a subtle, nonsignificant trend towards higher entropy was observed for responders versus nonresponders according to RECIST 1.1. We acknowledge that RECIST measurements are suboptimal as an outcome variable given the known limitations of RECIST to accurately assess response [29,30]. However, since the majority of study patients did not undergo resection of their liver metastases, correlation with histopathology was not feasible in our cohort and we chose RECIST as the main outcome as it is still most commonly used in clinical practice as well as in many previous study reports. Interestingly, our results are in line with a previous report of Rao et al. who did use histologic tumour regression grading (TRG) after surgery as the main outcome of response in a small group of 21 patients with CRLM and reported that – similar to our current findings – a non-significant trend towards higher entropy (without filter) in responders versus nonresponders. Rao et al. did find significant results when looking at relative changes in the texture measures after treatment with significantly decreased entropy compared to pre-treatment measurements in responders and increased entropy in nonresponders[13]. Ahn et al. found no significant difference in the pre-treatment entropy between responders and nonresponders to chemotherapy in a relatively large cohort of 235 patients with CRLM. However, they did describe a profile of other features (including skewness and standard deviation) that underlined the theory of a more heterogeneous imaging texture of liver metastases in responders versus nonresponders [31]. Altogether, the results of studies presented so far – including our own – appear to indicate a subtle but not (yet) strong role for pre-treatment textural assessment of CRLM to predict response.

When looking at previous results for whole-liver texture analysis, several studies describe higher entropy in the surrounding liver of patients with CRLM when compared to patients without metastases [15,16,32]. Moreover, Beckers et al. found that differences in the texture of the liver parenchyma can already be observed at the time of primary staging (when no visible lesions are apparent) in patients who develop metachronous metastases in the first 6 months after diagnosis, suggesting that liver texture may serve as a marker to predict the early course of disease [15]. Ganeshan et al. showed that CT texture analysis has potential to identify patients at risk for a reduced survival, based on lower entropy [33]. These findings were however described in a group of patients without metastases. Since our cohort only included patients in whom CRLMs were already present, these previously reported findings could not be explored in the current cohort. When it comes to whole-liver texture analysis for the prediction of the extent of disease, treatment response or survival we could not produce any significant findings.

There are some limitations to our study. First, the sample size is relatively small. Second, despite the standardised protocol, there were some differences between the scanners and slice thickness employed throughout this study, although a previous study suggested that scanner settings are of minor influence on the textural features [15]. Third, as already mentioned above, it was not possible to correlate our findings with underlying histopathology since most patients did not undergo resection of their CRLM. Fourth, in the subgroup undergoing chemotherapy, there were some variations in the chemotherapeutic regimen used. Finally, in the field of texture analysis, many features (derived from both first order as well as higher order statistical models) can be tested, which would result in a risk of false positive findings due to multiple testing (type I error). Therefore, for this study, we chose to only include a selection of first-order texture features commonly used in previous literature within the field of texture analysis in colorectal cancer to allow meaningful comparisons with previous evidence [15,18,32].

In conclusion, our study suggests that the ratio between the texture of liver metastases and the surrounding liver possibly reflects relevant changes in tissue microarchitecture and may be of value in the future to assess the extent of the disease in the liver and to predict overall survival.

References

[1] L.A. Torre, R.L. Siegel, E.M. Ward, A. Jemal, Global cancer incidence and mortality rates and trends–an update, Cancer Epidemiol. Biomark. Prev. 25 (1) (2016) 16–27.
[2] J. Leporrier, J. Maurel, L. Chiche, S. Bara, P. Segol, G. Launoy, A population-based study of the incidence, management and prognosis of hepatic metastases from colorectal cancer, Br. J. Surg. 93 (4) (2006) 465–474.
[3] S. Manfredi, C. Lepage, C. Hatem, O. Coatmeur, J. Faivre, A.M. Bouvier, Epidemiology and management of liver metastases from colorectal cancer, Ann. Surg. 244 (2) (2006) 254–259.
[4] A. Noren, H.G. Eriksson, L.I. Olsson, Selection for surgery and survival of synchronous colorectal liver metastases; a nationwide study, Eur. J. Cancer 53 (2016) 105–114.
[5] S. Bipat, M.C. Niekel, E.F. Comans, C.Y. Nio, W.A. Bemelman, C. Verhoef, J. Stoker, Imaging modalities for the staging of patients with colorectal cancer, Neth. J. Med. 70 (1) (2012) 26–34.
[6] M.C. Niekel, S. Bipat, J. Stoker, Diagnostic imaging of colorectal liver metastases with CT, MR, imaging, FDG PET, and/or FDG PET/CT: a meta-analysis of prospective studies including patients who have not previously undergone treatment, Radiology 257 (3) (2010) 674–684.
[7] E. Eisenhauer, P. Therasse, J. Bogaerts, L. Schwartz, D. Sargent, R. Ford, J. Dancey, S. Arbuck, S. Gwyther, M. Mooney, New response evaluation criteria in solid tumours: revised RECIST guideline (version 1.1), Eur. J. Cancer 45 (2) (2009) 228–247.
[8] P.J. Robinson, The effects of cancer chemotherapy on liver imaging, Eur. Radiol. 19 (7) (2009) 1752–1762.
[9] P. Therasse, S.G. Arbuck, E.A. Eisenhauer, J. Wanders, R.S. Kaplan, L. Rubinstein, J. Verweij, M. Van Glabbeke, A.T. van Oosterom, M.C. Christian, S.G. Gwyther, New guidelines to evaluate the response to treatment in solid tumors. European

Organization for Research and Treatment of Cancer, National Cancer Institute of the United States, National Cancer Institute of Canada, J. Natl. Cancer Inst. 92 (3) (2000) 205–216.
[10] G. Castellano, L. Bonilha, L.M. Li, F. Cendes, Texture analysis of medical images, Clin. Radiol. 59 (12) (2004) 1061–1069.
[11] M.G. Lubner, N. Stabo, S.J. Lubner, A.M. del Rio, C. Song, R.B. Halberg, P.J. Pickhardt, CT textural analysis of hepatic metastatic colorectal cancer: pre-treatment tumor heterogeneity correlates with pathology and clinical outcomes, Abdom. Imaging 40 (7) (2015) 2331–2337.
[12] K.A. Miles, B. Ganeshan, M.R. Griffiths, R.C. Young, C.R. Chatwin, Colorectal cancer: texture analysis of portal phase hepatic CT images as a potential marker of survival, Radiology 250 (2) (2009) 444–452.
[13] S.X. Rao, D.M. Lambregts, R.S. Schnerr, R.C. Beckers, M. Maas, F. Albarello, R.G. Riedl, C.H. Dejong, M.H. Martens, L.A. Heijnen, W.H. Backes, G.L. Beets, M.S. Zeng, R.G. Beets-Tan, CT texture analysis in colorectal liver metastases: a better way than size and volume measurements to assess response to chemotherapy? United Eur. Gastroenterol. J. 4 (2) (2016) 257–263.
[14] D. Caruso, M. Zerunian, M. Ciolina, D. de Santis, M. Rengo, M.H. Soomro, G. Giunta, S. Conforto, M. Schmid, E. Neri, A. Laghi, Haralick's texture features for the prediction of response to therapy in colorectal cancer: a preliminary study, Radiol. Med. 123 (March (3)) (2018) 161–167 Epub 2017 Nov 8.
[15] R.C.J. Beckers, D.M.J. Lambregts, R.S. Schnerr, M. Maas, S.-X. Rao, A.G.H. Kessels, T. Thywissen, G.L. Beets, S. Trebeschi, J.B. Houwers, C.H. Dejong, C. Verhoef, R.G.H. Beets-Tan, Whole liver CT texture analysis to predict the development of colorectal liver metastases—A multicentre study, Eur. J. Radiol. 92 (2017) 64–71.
[16] S.X. Rao, D.M. Lambregts, R.S. Schnerr, W. van Ommen, T.J. van Nijnatten, M.H. Martens, L.A. Heijnen, W.H. Backes, C. Verhoef, M.S. Zeng, G.L. Beets, R.G. Beets-Tan, Whole-liver CT texture analysis in colorectal cancer: does the presence of liver metastases affect the texture of the remaining liver? United Eur. Gastroenterol. J. 2 (6) (2014) 530–538.
[17] J.J. van Griethuysen, A. Fedorov, C. Parmar, A. Hosny, N. Aucoin, V. Narayan, et al., Computational radiomics system to decode the radiographic phenotype, Cancer Res. 77 (21) (2017) e104–e107.
[18] B. Ganeshan, K.A. Miles, R.C. Young, C.R. Chatwin, Hepatic entropy and uniformity: additional parameters that can potentially increase the effectiveness of contrast enhancement during abdominal CT, Clin. Radiol. 62 (8) (2007) 761–768.
[19] F. Davnall, C.S. Yip, G. Ljungqvist, M. Selmi, F. Ng, B. Sanghera, B. Ganeshan, K.A. Miles, G.J. Cook, V. Goh, Assessment of tumor heterogeneity: an emerging imaging tool for clinical practice? Insights Imaging 3 (6) (2012) 573–589.
[20] B. Ganeshan, K.A. Miles, Quantifying tumour heterogeneity with CT, Cancer Imaging 13 (2013) 140–149.
[21] C. Chen, L. Pau, P. Wang, The handbook of pattern recognition and computer vision, World Sci. (1998) 207–248.
[22] M.R. Weiser, W.R. Jarnagin, L.B. Saltz, Colorectal cancer patients with oligometastatic liver disease: what is the optimal approach? Oncology (Williston Park) 27 (11) (2013) 1074–1078.
[23] S. Holm, A simple sequentially rejective multiple test procedure, Scand. J. Stat. (1979) 65–70.
[24] B. Ganeshan, K. Skogen, I. Pressney, D. Coutroubis, K. Miles, Tumour heterogeneity in oesophageal cancer assessed by CT texture analysis: preliminary evidence of an association with tumour metabolism, stage, and survival, Clin. Radiol. 67 (2) (2012) 157–164.
[25] K. Hayano, N.M. Kulkarni, D.G. Duda, R.S. Heist, D.V. Sahani, Exploration of imaging biomarkers for predicting survival of patients with advanced non-small cell lung cancer treated with antiangiogenic chemotherapy, AJR Am. J. Roentgenol. 206 (5) (2016) 987–993.
[26] F. Ng, B. Ganeshan, R. Kozarski, K.A. Miles, V. Goh, Assessment of primary colorectal cancer heterogeneity by using whole-tumor texture analysis: contrast-enhanced CT texture as a biomarker of 5-year survival, Radiology 266 (1) (2013) 177–184.
[27] C. Yip, D. Landau, R. Kozarski, B. Ganeshan, R. Thomas, A. Michaelidou, V. Goh, Primary esophageal cancer: heterogeneity as potential prognostic biomarker in patients treated with definitive chemotherapy and radiation therapy, Radiology 270 (1) (2014) 141–148.
[28] H. Zhang, C.M. Graham, O. Elci, M.E. Griswold, X. Zhang, M.A. Khan, K. Pitman, J.J. Caudell, R.D. Hamilton, B. Ganeshan, A.D. Smith, Locally advanced squamous cell carcinoma of the head and neck: CT texture and histogram analysis allow independent prediction of overall survival in patients treated with induction chemotherapy, Radiology 269 (3) (2013) 801–809.
[29] Y.S. Chun, J.-N. Vauthey, P. Boonsirikamchai, D.M. Maru, S. Kopetz, M. Palavecino, S.A. Curley, E.K. Abdalla, H. Kaur, C. Charnsangavej, E.M. Loyer, Association of computed tomography morphologic criteria with pathologic response and survival in patients treated with bevacizumab for colorectal liver metastases, JAMA 302 (21) (2009) 2338–2344.
[30] W.S. Chung, M.S. Park, S.J. Shin, S.E. Baek, Y.E. Kim, J.Y. Choi, M.J. Kim, Response evaluation in patients with colorectal liver metastases: RECIST version 1. 1 versus modified CT criteria, AJR Am. J. Roentgenol. 199 (4) (2012) 809–815.
[31] S.J. Ahn, J.H. Kim, S.J. Park, J.K. Han, Prediction of the therapeutic response after FOLFOX and FOLFIRI treatment for patients with liver metastasis from colorectal cancer using computerized CT texture analysis, Eur. J. Radiol. 85 (10) (2016) 1867–1874.
[32] B. Ganeshan, K.A. Miles, R.C. Young, C.R. Chatwin, Texture analysis in non-contrast enhanced CT: impact of malignancy on texture in apparently disease-free areas of the liver, Eur. J. Radiol. 70 (1) (2009) 101–110.
[33] B. Ganeshan, K.A. Miles, R.C. Young, C.R. Chatwin, Hepatic enhancement in colorectal cancer: texture analysis correlates with hepatic hemodynamics and patient survival, Acad. Radiol. 14 (12) (2007) 1520–1530.
[34] D.G. Altman, P. Royston, The cost of dichotomising continuous variables, BMJ 332 (7549) (2006) 1080.